Deflection-Voltage Model and Experimental Results for Polymeric Piezoelectric C-Block Actuators

Andrew J. Moskalik* and Diann Brei†
University of Michigan,
Ann Arbor, Michigan 48109-2125

Introduction

THE smart structures field has grown rapidly over the last few years. One factor enabling this growth has been the development of small actuators based on smart materials such as piezoelectrics and shape memory alloys. Piezoelectric actuators are currently more widely used for smart structure applications because they are small, have low-power requirements, and respond quickly.[1] However, commonly used piezoelectric actuators produce either high force coupled with small deflections (stacks), or large deflections coupled with low force (bimorphs). For piezoelectric actuation, this leaves a gap in force–deflection capabilities in which many smart structures applications operate.

Recently, a variety of approaches have been proposed to fill this gap, including mechanical leveraging mechanisms,[2] moonie actuators,[3] Rainbow actuators,[4] and C-blocks.[5] The last of these, C-blocks, are curved piezoelectric bender actuators.

Prior research has demonstrated that C-blocks produce over 2.6 times the force of equivalent straight benders.[6] However, it is expected that this gain in force output is accompanied by some loss of deflection. The original research on these actuator architectures[5] was conducted using bimorph actuators fabricated from polyvinylidene fluoride (PVdF) polymer, which is an inherently weak material. To overcome this problem, the C-block actuator has evolved into a generic multilayered architecture, which has a stiffer structure than the bimorphs previously investigated. This C-block is a multilayered piezoelectric curved beam (shown in Fig. 1a) consisting of a variable number of active or inactive layers. The active layers are poled and electrically connected such that the layers above the neutral axis will strain opposite to those below the neutral axis. When a voltage is applied to the actuator the piezoelectric strains create a bending moment, which causes the actuator to flex as shown in Fig. 1b. To utilize these actuators for force improvement, the deflection must also be known. The steady-state deflection-voltage model for a generic individual C-block is presented and applied to three specific experimental test cases: a unimorph (one piezoelectric layer), a bimorph (two piezoelectric layers), and a multimorph (four piezoelectric layers).

Deflection-Voltage Theoretical Model

A simple theoretical deflection-voltage model for a generic actuator was derived using Hamilton's principle, similar to the approach used by Qatu[7] for nonpiezoelectric laminated curved beams. The nomenclature used in the derivation is shown in Fig. 2. To keep the resulting model simple, the C-block was assumed to be a thin, perfectly bonded, curved beam with a constant neutral axis radius R_n and a circumferential length of πR_n. To use Hamilton's principle, expressions for the internal stress and strain within the C-block were developed from the piezoelectric constitutive relation. With these stress and strain terms, the strain energy within the C-block was defined as the stress multiplied by the strain in each differential element and integrated throughout the volume of the C-block. The variation of the strain energy was used in Hamilton's principle to produce equations of equilibrium and the associated boundary conditions. The resulting governing differential equations are

$$\left(\frac{1}{\mathcal{X}}+1\right)u_{,\theta\theta}+\frac{1}{\mathcal{X}}w_{,\theta}-w_{,\theta\theta\theta}=0$$
$$u_{,\theta\theta\theta}-\frac{1}{\mathcal{X}}u_{,\theta}-\frac{1}{\mathcal{X}}w-w_{,\theta\theta\theta\theta}=\frac{N^P R_n^3}{D} \tag{1}$$

where u and w are the circumferential and radial displacements, respectively, and the subscript $,\theta$ indicates differentiation with respect to the angular coordinate θ. The nondimensional stiffness ratio $\mathcal{X}$, a measure of the thinness of the C-block, is defined in terms of the neutral axis and the composite stiffnesses as

$$\mathcal{X}=D/\left(AR_n^2\right) \tag{2}$$

where A and D are the composite extensional and bending stiffnesses, respectively, defined as

$$A=\sum_{i=1}^{q}Y_i b_i(z_i-z_{i-1}) \quad \text{and} \quad D=\sum_{i=1}^{q}\frac{1}{3}Y_i b_i\left(z_i^3-z_{i-1}^3\right) \tag{3}$$

Here, Y_i is Young's modulus of the ith layer, b_i is the width of the ith layer, and z_i is the distance to the neutral axis from the outside of the ith layer.

The piezoelectric normal force N^P in Eq. (1) and the internal piezoelectric moment M^P can be derived by integrating the piezoelectric stress across the cross-sectional area and are defined as

$$N^P=\sum_{i=1}^{q}Y_i b_i(z_i-z_{i-1})(d_{31}E_3)_i$$

and

$$M^P=\sum_{i=1}^{q}\frac{1}{2}Y_i b_i\left(z_i^2-z_{i-1}^2\right)(d_{31}E_3)_i \tag{4}$$

where d_{31} is the piezoelectric constant and E_3 is the applied electric field. The piezoelectric constant of nonpiezoelectric layers is assumed to be zero.

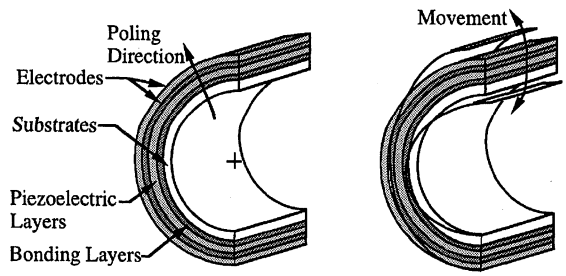

a) C-blocks are curved, multilayered piezoelectric actuators constructed of a variable number of layers

b) Piezoelectric strain produces an internal moment, causing the C-block to flex

Fig. 1 C-block design and operation.

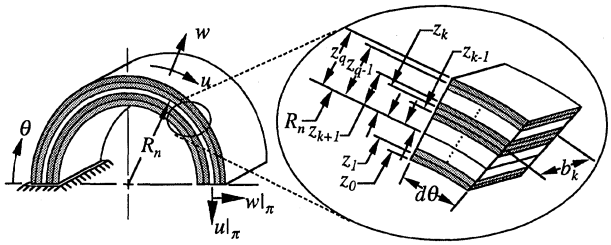

Fig. 2 Nomenclature for an individual C-block: R_n is the radius to the neutral axis; z is the distance from the neutral axis; b is the width; u and w are circumferential and radial displacements, respectively; and θ is the angular coordinate.

Received Dec. 15, 1995; revision received June 3, 1997; accepted for publication June 9, 1997. Copyright © 1997 by the American Institute of Aeronautics and Astronautics, Inc. All rights reserved.

*Graduate Student, Department of Mechanical Engineering and Applied Mechanics, 2250 G. G. Brown.

†Assistant Professor of Mechanical Engineering, Department of Mechanical Engineering and Applied Mechanics, 2250 G. G. Brown. Member AIAA.

The corresponding boundary conditions developed for the C-block from Hamilton's principle are

$$\begin{aligned} &\left[\left(D/R_n^2\right)(-w_{,\theta\theta} + u_{,\theta}) + M^P\right]_\pi = 0 \\ &\left[\left(D/R_n^3\right)(-w_{,\theta\theta\theta} + u_{,\theta\theta})\right]_\pi = 0 \\ &\left\{\left[D/\left(\chi R_n^3\right)\right](u_{,\theta} + w) + N^P\right\}_\pi = 0 \end{aligned} \tag{5}$$

at the free end, where $\theta = \pi$, and

$$w|_0 = 0, \qquad w_{,\theta}|_0 = 0, \qquad u|_0 = 0 \tag{6}$$

at the clamped end, where $\theta = 0$.

The equations of equilibrium [Eq. (1)] and associated boundary conditions [Eqs. (5) and (6)] were solved to determine the final quasistatic deflection-voltage model for the deflection of the C-block

$$w = \left(\frac{N^P R_n^3 \mathcal{X}}{D} - \frac{M^P R_n^3}{D}\right)(1 - \cos\theta) \tag{7}$$

This model can be further simplified by introducing two assumptions. First, the deflection at the tip, which is the point used most for actuation purposes, is the point of interest. Therefore, Eq. (7) is evaluated at the tip, where $\theta = \pi$. Second, because the C-block is thin, the nondimensional stiffness ratio $\mathcal{X}$ is much smaller than one. When the C-block is constructed as a bender, i.e., the moment term M^P is not canceled due to symmetric construction, the normal force term $N^P R_n \mathcal{X}$ is much smaller than the corresponding moment term M^P. Therefore, this term in Eq. (7) can be assumed to be small and neglected. With these considerations, the static relation between the radial deflection $w|_\pi$ and the voltage V becomes

$$\begin{aligned} w|_\pi &= \frac{2M^P R_n^2}{D} \\ &= -\frac{3R_n^2 \sum_{i=1}^q b_i Y_i (d_{31}V)_i \left(z_i^2 - z_{i-1}^2\right)/(z_i - z_{i-1})}{\sum_{i=1}^q b_i Y_i \left(z_i^3 - z_{i-1}^3\right)} \end{aligned} \tag{8}$$

where the piezoelectric moment M^P and the composite bending stiffness D have been expanded using Eqs. (3) and (4), respectively.

Experimental Case Studies

To verify that the theoretical deflection-voltage model [Eq. (8)] accurately predicts the quasistatic deflection behavior of physical prototypes, three experimental case studies were conducted: a unimorph (one active piezoelectric layer with substrate), a bimorph (two active layers), and a multimorph (four active layers). Cross sections of the prototypes used in these case studies are shown in Fig. 3. The unimorph configuration (Fig. 3a) was chosen because it is not symmetric about the neutral axis and, thus, contains a piezoelectric normal force term N^P. The bimorph configuration (Fig. 3b) was chosen because it is the simplest symmetric case, and this standard configuration can be compared directly to conventional bimorphs. The multimorph (Fig. 3c) was chosen to ascertain the effect of a multilayered structure. A four-layer multimorph was the simplest configuration to build that had more than one active layer on each side of the neutral axis.

Prototype Fabrication

To fabricate each prototype, PVdF films were bonded together in the configurations shown in Fig. 3. After being epoxied, the films were molded into a semicircular shape by wrapping them around a cylindrical dowel. Once the epoxy had cured, the base of the C-block was secured between glass slides and lead wires were connected with conductive copper tape. To eliminate arcing across the thin bonding layer, prototypes were constructed with the poling directions aligned such that adjacent electrodes had the same potential.

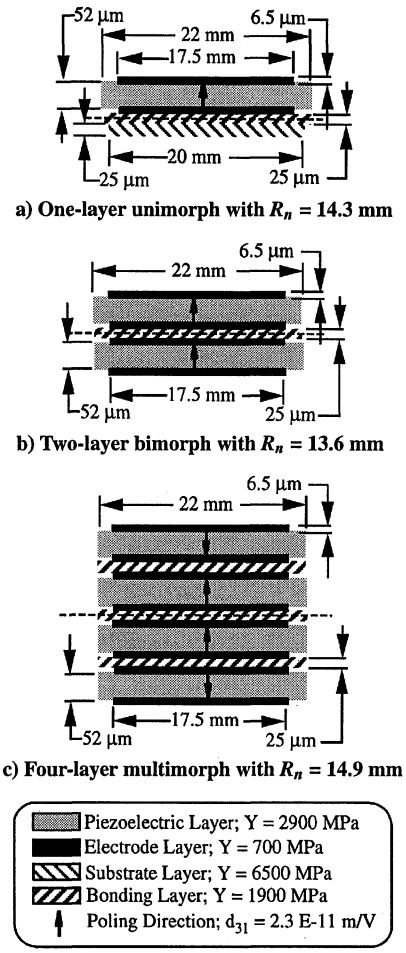

Fig. 3 Cross-sectional description and notation for three tested case studies.

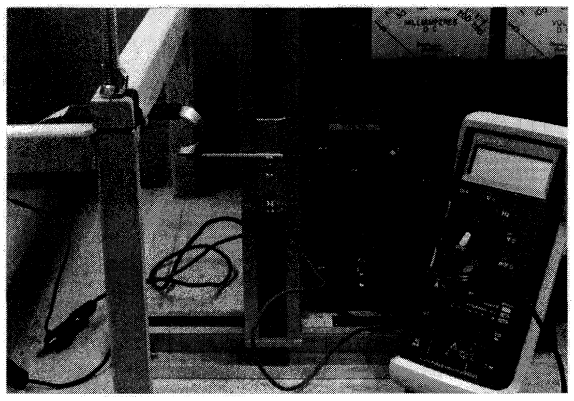

Fig. 4 Experimental apparatus for deflection-voltage experiments: the prototype was clamped in place and connected to a high-voltage power supply; the voltage was incremented, and the tip deflection was tracked using a calibrated scale.

Experimental Apparatus and Procedure

The laboratory setup used for all experiments is shown in Fig. 4. Each prototype was clamped in place so that the radial tip movement of the C-block was in the vertical direction. The lead wires from the prototype were connected directly to a high-voltage power supply, which was monitored with a digital multimeter. The position of the tip of the C-block was tracked with a pointer attached to a calibrated scale.

For each of these prototypes a similar experimental procedure was executed. The initial position of the tip of the prototype was recorded with the calibrated scale. Voltage was then applied to the prototype in increments of 10 V starting with 0 V and ending with 400 V. The voltage was then lowered, again in 10-V increments, back to 0 V. At each increment the position of the tip of the prototype was

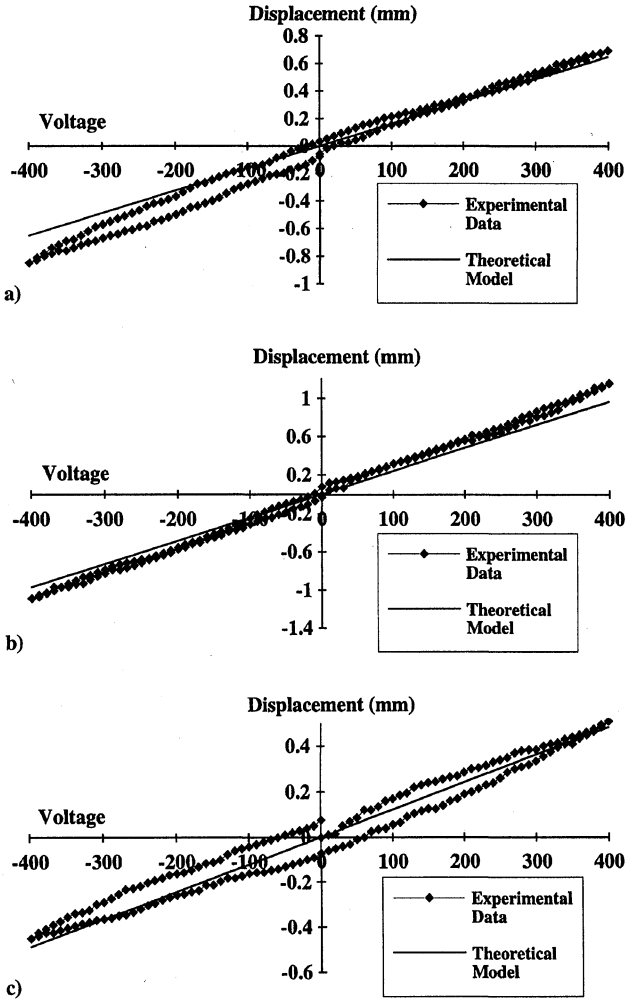

Fig. 5 Deflection-voltage experimental results: three prototypes tested showed differences in deflection between the theoretical model and the experimental data of 0.068 mm for the unimorph, 0.80 mm for the bimorph, and 0.048 mm for the multimorph.

measured and the displacement calculated. Once the voltage was lowered to 0 V, the leads were reversed to give a negative voltage input. The voltage was then increased in −10-V increments from 0 to −400 V and back up to 0 V again, recording the displacement at each increment.

Deflection-Voltage Experimental Results

The experimental results and the behavior predicted by the deflection-voltage theoretical model are shown in Fig. 5 for each case study. All experimental results tend to follow a hysteresis curve around the theoretical model; this is most noticeable in the graph for the multimorph. Hysteresis is common in piezoelectric actuators but, to keep the theoretical model as simple as possible, it was not accounted for in the model derivation. Note that the data points begin to diverge from the expected curve at high voltages. This could be due to nonlinear effects of the piezoelectric material and/or large radius changes in the C-block, neither of which was accounted for in the model. The mean differences between the experimentally observed behavior of the prototypes and the theoretical model were 0.048 mm for the multimorph, 0.068 mm for the unimorph, and 0.080 mm for the bimorph. This corresponds to errors ranging from 8.3 to 10.4% of the full-scale theoretical predictions. Thus, despite the nonlinear effects and other sources for error, the observed behavior of each prototype agrees well with the behavior predicted by the simple models.

Conclusion

This Note presented a simple steady-state theoretical deflection-voltage model for a generic individual C-block. This model was derived by solving the equations of equilibrium and boundary conditions obtained from Hamilton's principle. The theoretical model was verified by fabricating and testing three experimental case study prototypes: a unimorph, a bimorph, and a four-layer multimorph.

The experimental case studies demonstrate a good overall correlation with the theoretical model. The experimental results for each case study agree within 11% with the behavior predicted by the deflection-voltage model. The unimorph case study showed no more error than the other case studies; therefore, it can be concluded that the normal force term in Eq. (7) is small compared to the moment term. As expected, nonlinear effects such as hysteresis were observed in all of the experiments. These effects were not included in the theoretical derivation to minimize the complexity of the resulting model. The inclusion of additional layers in the multimorph results in a stiffer structure and, thus, the deflection decreases approximately linearly [Eq. (8)] as both the piezoelectric moment and the stiffness increase. However, the stiffer multimorph produces more force, offsetting the loss in deflection. Therefore, there is a design tradeoff between force and deflection output, which is a topic currently under research.

The theoretical deflection-voltage model for the C-block can be used to compare the C-block architecture to a conventional straight bender. Comparing Eq. (8) to the deflection of a straight bender, the C-block produces 0.405 times the output deflection of an equivalent straight bender. However, it has been shown that the C-block produces 2.66 times the output force of an equivalent straight bender.[6] Therefore, the C-block produces 8% more work that the conventional bender, demonstrating the C-block's potential as a more efficient architecture.

Acknowledgments

The authors would like to thank the Army Research Office (Grant DAAH04-96-1-0186) and the National Science Foundation (Grant CMS-952637) for supporting this research.

References

[1]Damjanovic, D., and Newnham, R. E., "Electrostrictive and Piezoelectric Materials for Actuator Applications," *Journal of Intelligent Material Systems and Structures*, Vol. 3, No. 2, 1993, pp. 190–208.

[2]Bamford, R., Kuo, C. P., Glaser, R., and Wada, B. K., "Long Stroke Precision PZT Actuator," *Proceedings of the AIAA/ASME/ASCE/AHS/ASC Structures, Structural Dynamics, and Materials Conference*, AIAA, Washington, DC, 1995, pp. 3278–3284.

[3]Onitsuka, K., Dogan, A., Tressler, J. F., Xu, Q., Yoshikawa, S., and Newnham, R. E., "Metal-Ceramic Composite Transducer, the 'Moonie'," *Journal of Intelligent Material Systems and Structures*, Vol. 6, No. 4, 1995, pp. 447–455.

[4]Haertling, G. H., "Ultra-High-Displacement Actuator," *American Ceramic Society Bulletin*, Vol. 73, No. 2, 1994, pp. 93–96.

[5]Brei, D., "Force-Deflection Behavior for C-block Piezoelectric Actuator Architectures," *Smart Structures and Materials 1995: Smart Structures and Integrated Systems*, edited by I. Chopra, *Proceedings of the SPIE*, SPIE 2443, Society of Photo-Optical Instrumentation Engineers, Bellingham, WA, 1994, pp. 362–373.

[6]Moskalik, A., and Brei, D., "A Novel PZT Bender with Enhanced Force-Voltage Performance," *Society of Engineering Science 33rd Annual Technical Meeting Book of Abstracts*, Society of Engineering Science, Tempe, AZ, 1996, p. FD2.

[7]Qatu, M. S., "Theories and Analyses of Thin and Moderately Thick Laminated Composite Curved Beams," *International Journal of Solids and Structures*, Vol. 30, No. 20, 1993, pp. 2743–2756.

G. A. Kardomateas
Associate Editor